



Control of fracture networks on a coastal karstic aquifer: a case study from northeastern Yucatán Peninsula (Mexico)

Juan Carlos Zamora-Luria^{1,2} · Jorge Adrián Perera-Burgos³ · Alfredo González-Calderón⁴ · Luis E. Marin Stillman¹ · Rosa Ma. Leal-Bautista¹

Received: 14 February 2020 / Accepted: 1 September 2020 / Published online: 1 October 2020
© Springer-Verlag GmbH Germany, part of Springer Nature 2020

Abstract

The Yucatán Peninsula karst aquifer in southeastern Mexico is important because it is the only source of freshwater supply in the region. Along the eastern coast, the aquifer behaves as a shallow unconfined aquifer, and one of its main characteristics is the development of a complex network of karstic conduits. Electrical resistivity tomography (ERT) is a geophysical technique that provides reliable information on aquifer properties that can be applied to karst. With this in mind, ERT surveys (with dipole-dipole and Wenner arrays) together with vertical profiles of groundwater electrical conductivity were obtained in the northeast of Yucatán Peninsula in the Akumal zone. The objective was to evaluate the characteristic structure of the unsaturated and saturated areas, and to determine the importance of factors at a local level that affect the thickness of the freshwater lens, as well as groundwater flow directions near the coast. The results of the ERT sections show a thin vadose zone with resistivity values greater than 1,052 Ωm and a saturated zone with resistivity values that vary from 1 to 1,052 Ωm , and show the presence of dissolution conduits and fracture zones that are affecting the freshwater lens of the aquifer. In addition, water-table measurements show the role of fracture networks in the groundwater flow. The overall results indicate conditions for a possible microbasin in the Akumal zone, highlighting the importance of local fractures, which could work as groundwater divides along the eastern coast of the Yucatán Peninsula.

Keywords Karst · Coastal aquifer · Geophysical methods · Groundwater flow · Mexico

Introduction

Karst aquifers are vitally important because they provide freshwater to 25% of the world's population (Ford and Williams 2007). These aquifers have unique and complex characteristics that make them different from intergranular

porosity aquifers; thus, the study methods used in other fields of hydrogeology (well monitoring, pumping tests and distributed models) provide limited information (Bakalowicz 2005).

In Mexico, karst areas occur in 20% of the national territory, and the Yucatán Peninsula aquifer is the most relevant in this regard. This karst aquifer is one of the largest aquifers in the world, and the only source of freshwater for the population of this region; in addition, it has an impact on regional finances and it is an international tourist attraction. The Yucatán Peninsula aquifer has an extension area of about 165,000 km², covering the states of Campeche, Yucatán and Quintana Roo (CONAGUA 2002).

The most studied area of the Yucatán Peninsula karst aquifer is the region near the Ring of Sinkholes or Chicxulub crater, in which a wide variety of geological (Rebolledo-Vleyra et al. 2010; Schulte et al. 2010), geophysics (Andrade-Gómez et al. 2019; Gómez-Nicolás et al. 2017; Zhu et al. 2011) and hydrogeological studies (Escolero et al. 2005; Marín et al. 2004; Perry et al. 2002; Rebolledo-Vieyra et al. 2011) have been developed.

Currently, there are only a few geological and geophysical studies carried out in other areas of the Yucatán Peninsula,

✉ Rosa Ma. Leal-Bautista
rleal@cicy.mx

¹ Unidad de Ciencias del Agua, Centro de Investigación Científica de Yucatán, A.C, Calle 8, No. 39, Mz. 29, S.M. 64, C.P, 77524 Cancún, Quintana Roo, Mexico

² Present address: Universidad del Caribe, Lote-1, Manzana 1, Esquina Fraccionamiento Tabachines, Super Manzana 78, CP 77528, Cancún, Quintana Roo, Mexico

³ CONACYT - Unidad de Ciencias del Agua, Centro de Investigación Científica de Yucatán, A.C, Calle 8, No. 39, Mz. 29, S.M. 64, C.P, 77524 Cancún, Quintana Roo, Mexico

⁴ CONACYT - CIDESI sede Campeche, Carretera Carmen Puerto Real km 7.5, Mundo Maya, C.P. 24153, Cd. del Carmen, Campeche, Mexico

most of them concentrated in the southern area of the Mexican Caribbean (Gondwe et al. 2012; Ochoa-Tinajero 2016; Saint-Loup et al. 2018; Schiller et al. 2017). The lack of petrophysical information together with a high heterogeneity of the aquifer system, can cause biases in the interpretation of hydrogeological behavior, which has already been noted by Gondwe et al. (2011) in their modeling study of the aquifer in the Sian Ka'an biosphere reserve in Quintana Roo. Obtaining this type of information is vital for developing studies on numerical modeling (Hartmann et al. 2014; Medici et al. 2019) and intrinsic vulnerability of groundwater in karst systems (Wachniew et al. 2016).

In general, karst systems are known to be highly sensitive and vulnerable to human activities such as tourism, agriculture, and the creation of new urban centers, and the aquifer of the Yucatán Peninsula is no exception (Leal-Bautista et al. 2013; Saint-Loup et al. 2018). With regard to the increment in population, the Mexican Caribbean presents the highest growth rate in Mexico, notably Playa del Carmen, the fastest growing city in the country (Hernández-Terrones et al. 2015). Currently, development plans by the State of Quintana Roo include the construction and/or growth of small villages to provide small urban centers—for example, the case of Akumal, which has a current population of 1,310 inhabitants (INEGI 2010) that is estimated to increase up to 130,000 by 2030 (Akumal 2007). Hernández-Terrones et al. (2015) reported that there is an increase in pollution in this area due to groundwater discharges and poor water treatment systems. In addition, there is little information on the status of the aquifer in this area, especially on the thickness of the freshwater lens and on the phenomena of saline intrusion; therefore, this information is of vital importance for developing a sustainable groundwater distribution plan.

One way to obtain information about this karst aquifer is through geophysical surveys, specifically the electrical resistivity tomography (ERT) technique, which is based on the subsurface response of the underground materials when an electric current is injected. It has been widely used in the study of karst systems (Gómez-Nicolás et al. 2017; Redhaounia et al. 2016; Zhu et al. 2011) and in saline intrusion studies (Galazoulas et al., 2015; García-Menéndez et al. 2018; Goebel et al. 2017, 2018). Due to the high resistivity of carbonated rocks, the conductivity of the subsoil in karst aquifers is mainly due to the electrolytic conduction of the interstitial fluid (Stummer et al. 2004), thus there is a marked contrast in the resistivity of the rock when it is saturated by freshwater or saline water. Minsley et al. (2011) demonstrated that it is possible to differentiate an area saturated with freshwater from an area saturated with saline water using ERT.

The aim of this work was to evaluate the structural characteristics of the unsaturated and saturated areas of the Akumal aquifer and to determine the importance of factors at a local level that affect the thickness of the freshwater lens as well as

groundwater flow directions near the coast. To address this research goal, ERT surveys were used together with measurements of groundwater electrical conductivity (EC) in deep water columns. In addition, water-table measurements were made to assess the direction of groundwater flows by determining hydraulic gradients. The results of this work will allow development of a conceptual model at a more specific scale based on accurate information of the state of the aquifer. Furthermore, the information generated is vital for the development of numerical models of groundwater flows, as well as for vulnerability studies of the water resource.

Geological and hydrogeological framework of the Yucatán Peninsula

The Yucatán Peninsula is the emerging part of the Yucatán platform, and is characterized by a base of rocks of igneous and metamorphic origin of the Paleozoic, on which has evolved a sequence of calcareous sediments with thicknesses ranging from 1,500 m to more than 3,000 m (López-Ramos 1975; Weidie 1985), consisting of limestone, dolostone and evaporite rocks. The exposed rock is in a range of geological ages from the Upper Cretaceous to the Holocene with a trend of younger carbonates deposited on the margins, forming strata that are almost horizontal throughout the peninsula (López-Ramos 1975; Schönian et al. 2005).

The oldest carbonates are found in the northwestern part of the peninsula—these are highly permeable and reach thicknesses of up to 1,000 m in the area near the city of Merida, while on the Caribbean coast they reach thicknesses of up to 150 m, up to 50 km inland (Gondwe and Rahbek 2007). According to Weidie (1985) the eastern part of the Yucatán Peninsula is made up of carbonates that were deposited in the Pleistocene due to the transgression of the sea, and which extend up to a distance of 10 km inland.

The main structural axes of the Yucatán Peninsula have a west–northwest–southeast and north–northeast–southeast orientation and are associated with the *Sierrita de Ticul* and the Bacalar Río Hondo System, respectively (Bonet and Butterlin 1962). The axis determined by the *Sierrita de Ticul* corresponds to a normal type fault. The Bacalar Río Hondo System is a series of normal stepped faults, forming horst and graben features that vary in length and displacement. There is a set of fractures that, like *Sierrita de Ticul* and the Bacalar Río Hondo System, is of great importance. These fractures are known as the Holbox Fracture Zone, ranging from Cape Catoche to Holbox (López-Ramos 1975; Marín et al. 2000).

The carbonates of the Yucatán Peninsula are highly karstified, which has given rise to one of the longest flooded cave systems in the world, located in the state of Quintana Roo (Supper et al. 2009). In this state is located one of the five physiographic regions of the peninsula, the so-called “Eastern

Fault Block District” (Isphording 1974). The biggest fracture in this region is the fracture of Holbox-Xel Ha, which originates on the northeast coast of the peninsula to the south with a trend N5°E and N10°E (Bauer-Gottwein et al. 2011). Fracture expressions occur on the surface with polje depressions which, depending on the season, may be covered with water (Weidie 1978). According to Tulaczyk et al. (1993) this area is highly permeable and has a great influence on groundwater flow on a regional scale.

The Yucatán Peninsula karst aquifer behaves in most of its extension as an unconfined aquifer, where there is no flow at the surface because the soil in the area is thin and, in some areas, null (Beddows 2003). In addition, the surface rock is highly fractured so there is a rapid infiltration of meteoric water into the aquifer. This aquifer is shallow, with a water-table depth that varies from 2 m in the coastal area, to more than 20 m inland (QRSS 2013). The hydraulic gradient is low, with variations of 3–7 cm/km in Pliocene age areas (Gondwe et al. 2010a, b). The low potential of the hydraulic gradient is attributed to water-table depressions caused by the dissolution conduits that concentrate groundwater flow (Ford and Williams 2007) and can reach densities of 2 km/km² on the Mexican Caribbean coast (Beddows 2003). The saturation thickness of this aquifer increases as the distance to the coast increases.

The best-known hydrogeological regional model of the aquifer indicates that coastal areas present the saline intrusion effect, with a freshwater lens floating over greater-density saline water, which gives rise to the formation of a halocline, the thickness of which depends on geological characteristics and underground flow rates. In studies conducted by Beddows (2003) and Beddows et al. (2007), it is reported that at distances between 0.4 and 10 km from the coast, the depth of the halocline is less than that predicted by the Ghyben-Herzberg (GH) relationship. On the other hand, Gondwe et al. (2010a, b); report that this relationship operates on a regional scale.

Study area

The study area is located in the Akumal zone, located on the east coast of Quintana Roo state, approximately 35 km south of Playa del Carmen and 27 km north of Tulum (Fig. 1). This area is located in the hydrogeological unit called *Planicie Interior*, according to the administrative considerations of the National Water Commission (CONAGUA 2002).

The stratigraphy of the area corresponds to the Carrillo Puerto Formation (López-Ramos 1975). Coastal carbonates belong to the upper, middle and lower Pleistocene, and are presented in marine and nonmarine sequences accumulated on the margin of the platform due to the transgression of the sea (Lauderdale et al. 1979; Perry et al. 1995). Marine sequences include coastal strata, lagoons and coral reef limestones; the

rest of the geological material consists of eolianites, freshwater-lake carbonates, and recrystallized carbonates known locally as caliche (Kambesis and Coke IV 2013). Underlying the Pleistocene strata are the carbonate rocks of the Miocene-Pliocene (Richards and Richards 2007).

The area between Akumal and Tulum is highly fractured, where these fracture sets along the entire coast have a well-defined fracture trend (N50–60°W). There is also a second set of fractures which is parallel to the coast with a trend of N30–40°E. The fracture sets may form an orthogonal system that is genetically related to the Rio Hondo Fault Zone (Weidie 1978).

The annual average rainfall in the area is 1,464 mm, which occurs mainly from May to October and from June to December, where natural phenomena occur as hurricanes, depressions, and tropical storms. The average annual temperature is 26 °C (CONAGUA 2014).

Methodology

To characterize the karst aquifer in the Akumal area, ERT surveys were made and vertical profiles of groundwater EC were performed in depth water columns as an underground truth technique, which allowed ERT measurements to be calibrated. Three field campaigns were carried out during the month of May 2018, within the dry period at the Yucatán Peninsula. The results obtained were correlated with each other in order to assess local fracture conditions and their influence on underground flow such as the thickness of the freshwater lens in relation to the distance from the coast. Figure 2 shows specific sites for EC profiles, ERT measurements and water-table measurements.

EC profiles and water level measurements

EC profiles were measured in two water columns, of an observation well (W3) and a sinkhole (C3), using CastAway-CTD equipment (SonTek Xylem, San Diego, CA, USA) with a salinity and temperature accuracy of 0.1 PSU and 0.05 °C, respectively, and a depth resolution of 0.01 m. The depth of the water columns allowed the identification of the saturated areas of the aquifer, i.e. the thickness of zones saturated with freshwater, saltwater and the mixing zone or halocline. Depth to the water table and hydraulic head measurements were performed using a differential global positioning system (GPS; R8s Trimble), with an accuracy of 15 mm vertically; in some cases, it was necessary to use a water level probe (model 101 Solinst), with a precision of ±1 mm. The measurement sites were identified with the following nomenclature—W1, W2 and W3, wells in Uxuxubi; L1 and L2, lagoons in Uxuxubi; and S1 and S2, sinkholes in the village of Akumal. The spatial configuration of the water level measurements, with respect to ERT transects, is clearly seen in Fig. 2.

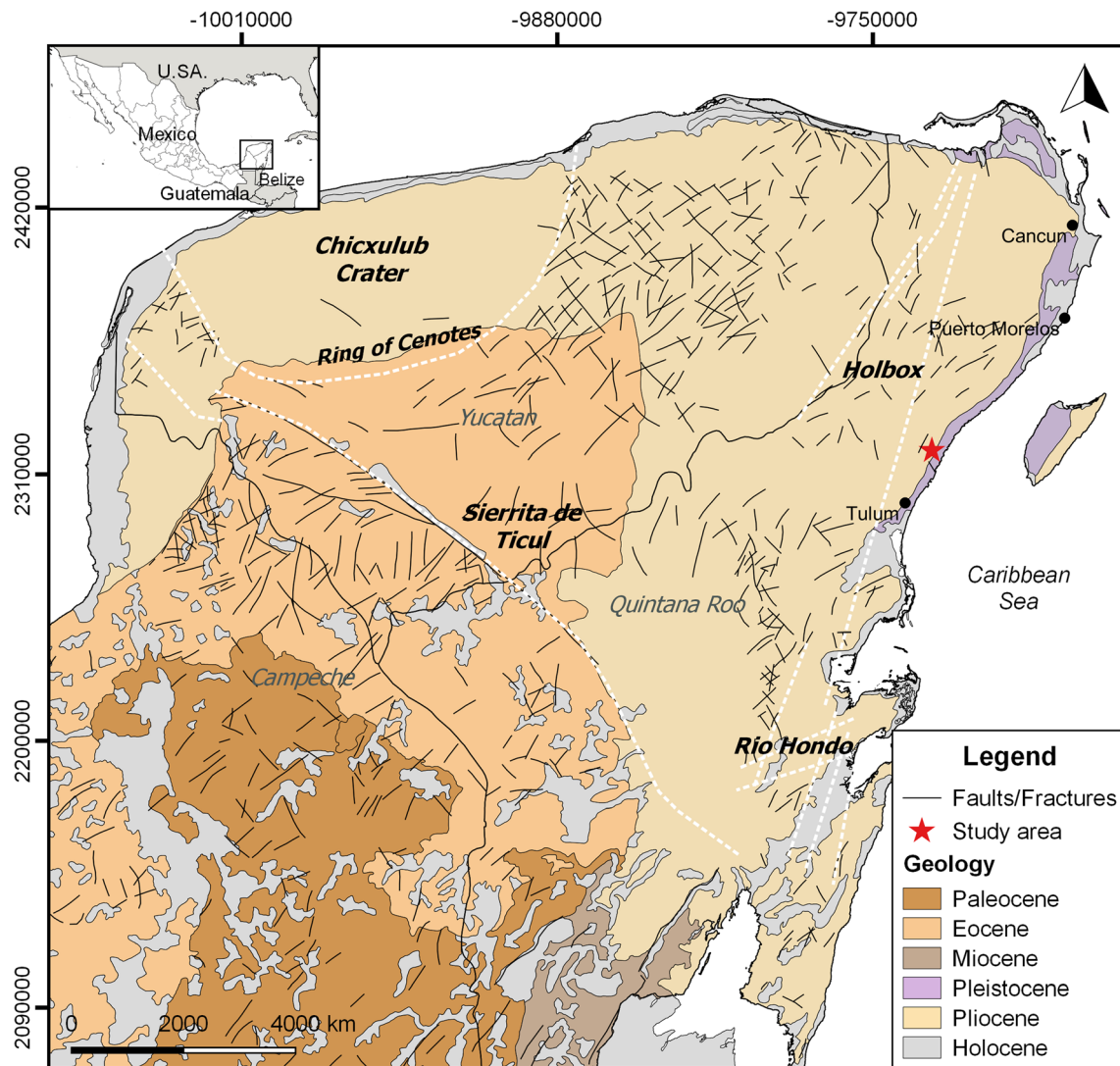


Fig. 1 Geological map of the Yucatán Peninsula (SGM 2006). Background colors indicate the age of the surface geology. While the main regional-scale fractures (dashed white line) are the most notable features at the Yucatán Peninsula, the small fractures (black lines) have been less studied

Electrical resistivity tomography measurements

Electrical resistivity tomography measurements were obtained using Super-Sting R1/IPA AGI (Advances Geosciences Inc., Austin, Texas) equipment. The spatial configuration of these transects (T1–T8) was designed with accessibility to the measurement sites (roads and vegetation-free zones) in order to cover as much area as possible within the study area (see Fig. 2). In all, 70 stainless steel electrodes were used, with a spacing of 5 m, thus covering a total length of 345 m per transect. Since the objective of the work was to evaluate the structural characteristics of the unsaturated and saturated areas of the aquifer, dipole-dipole (T1, T4, T5, T6) and Wenner (T2, T3, T7, T8) arrays were used. The dipole-dipole array was used because it is most sensitive to subvertical features in any kind of

geology, including karst areas and has a greater depth of investigation compared to other arrays. By using this array, it was possible to see if the lateral changes were significant in the aquifer (Sharma and Verma 2015). The Wenner array was used because it is better at resolving vertical changes, i.e. it is better at detecting the freshwater–saltwater interface. By using this array, it was possible to detect the vadose zone, freshwater and saltwater (Zhou et al. 2000). Both arrays were used at the three sites of the study area, Uxuxubi, Chemuyil and Akumal, as is shown in Fig. 2.

Although not accounting for topography may result in distorted resistivity results, the impact of such effects is known to be considerably lower at sites with topographic slopes less than 10° (Doro et al. 2013; Plank and Polg 2019; Telford et al. 1990). Topography measurements were carried out to identify

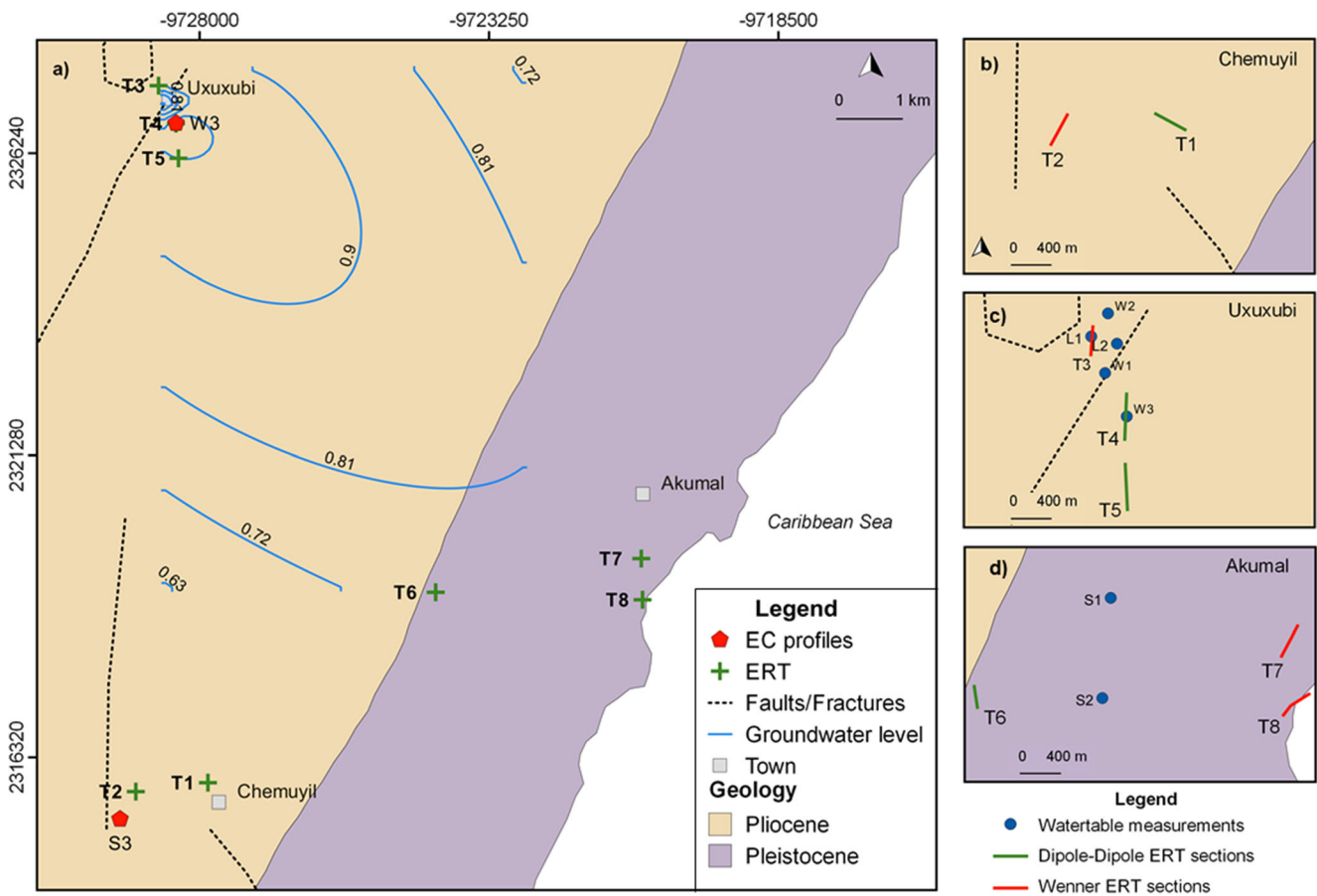


Fig. 2 a Sites and transect locations at the study area. Background colors show the age of surface geology. The youngest exposed sediments can be observed along the beach line. Maps (b–d) show the position of the transects and their real orientations

irregularities of the terrain where transects were located. However, these were not included in the inversion process since the terrain where transects were acquired was flat with a low slope. Prior to each measurement, a contact resistance test was performed according to the criteria given by Advanced Geosciences Inc. (2011).

Description of the inversion process for the ERT

The apparent resistivity sections obtained in each transect were inverted by EarthImager 2D v2.4.0 software (Advanced Geosciences Inc. 2005) to obtain the geo-electric sections of actual subsurface resistivity. The inversion process was carried out in three stages: (1) parameter adjustment, (2) direct modeling and (3) resistivity inversion. For the adjustment of parameters, filters recommended by Gómez-Nicolás et al. (2017) for a karst area of the Yucatán Peninsula were used, i.e. data with voltages less than 0.2 mV, resistivity less than 0.01 m and resistivity greater than 10^5 m. For direct modeling, the finite element method with a Cholesky factorization was used together with Dirichlet-type boundary conditions. Finally, for the inversion process, a smooth model

inversion was used, also known as Occam's inversion (Constable et al. 1987). The depth of investigation of each transect was calculated based on the measurements themselves. In some cases, a cutoff depth was set for the inversion of the ERT profiles, in order to reduce the root mean square (RMS) error, which is an indicator of the differences between the observed data (apparent resistivity) and those calculated in the inversion process (real resistivity).

The interpretation of the geo-electrical sections was made based on a comparison of the resistivity values obtained from the inversion process, with resistivity values reported for other areas of the Yucatán Peninsula karst aquifer where the same ERT technique was used (Andrade-Gómez et al. 2019; Gómez-Nicolás et al. 2017; Ochoa-Tinajero 2016).

Results

Water-table depth and freshwater-lens thickness

Two vertical profiles of groundwater EC were obtained showing the saturated areas of the aquifer. Profile W3,

corresponding to the observation well, was located at a perpendicular distance of 5 m from the middle section of the T4 transect, and at 10 km from the coast. The S3 profile, corresponding to the Chemuyil sinkhole, was located 50 m parallel to the start of the T2 transect, and at 6 km from the coast (Fig. 3). The depth to the water table with respect to the terrain surface was 4.774 m for W3 and 10.96 m for S3.

According to the profile S3 (Fig. 3), the thickness of the freshwater lens 6 km from the coast is approximately 17 m, with a halocline 5 m thick, and below it, seawater, which has a salinity of 35 PSU. At 10 km from the coast, according to the profile W3, a thickness of the water lens of 25 m is observed, with a halocline of 5 m thick. As can be seen from both measurements, the thickness of the halocline is the same at these sites. Although both measurements are not enough to confirm that the thickness of the halocline remains constant up to a distance of 10 km from the coast, there are reports where it is mentioned that the latter maintains a constant thickness in areas with a high hydraulic conductivity (Kovacs et al. 2017a, b; Moore et al. 1992). In addition, a gradual increase in the thickness of the freshwater lens is observed as the distance to

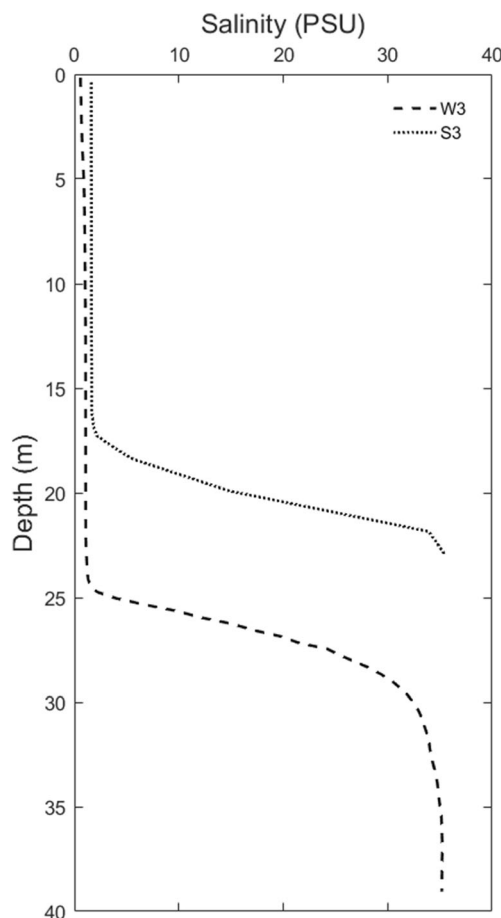


Fig. 3 Electrical conductivity (salinity) profiles. Notice the freshwater lens thickness, the halocline and the saline water presence in the aquifer. W3 profile (dashed line) was located at 10 km from the coastline, whereas S3 profile (dotted line) at 6 km

the coast increases, as it has been observed in other coastal areas of the Yucatán Peninsula aquifer (Beddows et al. 2007).

Hydraulic head values obtained in all sites are presented in Table 1. Water levels indicate a low hydraulic gradient, with a local groundwater flow to the Uxuxubi site, and on a larger scale, a groundwater flow towards the coast. Isolines from these measurements can be seen in Fig. 2.

It is important to mention one point regarding groundwater measurements. These are representative of the period in which they were measured (dry period), so their extrapolation to other periods of the year should be taken with caution, since it is well known that hydrological forcings such as aquifer recharge (Marino 1974), extreme weather effects—such as storms and hurricanes (Coutino et al. 2017; Kovacs et al. 2017a, b); types of tides (Canul-Macario et al. 2020; Levanon et al. 2017; Vera et al. 2012); and also sea-level rise (Katabchi et al. 2016)—can alter water levels and seawater intrusion in coastal aquifers. However, in other areas of the Yucatán Peninsula, water level variations of less than 1 m have been measured without taking into account extreme weather effects (Vera et al. 2012).

ERT geophysical surveys

Figures 4 and 5 presented the inverted two-dimensional (2D) sections for ERT measurements made in the study area. Noticeable, the resistivity values of the aquifer have a range of variation of 1 to 35,000 Ωm . High resistivity values are associated with the unsaturated zone, while the lower values are associated with the saturated zone of the aquifer. The variation in the resistivity values, which can be observed with the color scale, allowed one to identify the saturated area with values from 1 to 1,052 Ωm (green-blue colors) and the unsaturated area of the aquifer with values greater than 1,052 Ωm (red-yellow colors), which are in a good agreement with results of other karstic areas (Gómez-Nicolás et al. 2017; Redhaounia et al. 2015; Tassy et al. 2014).

The conceptual resistivity model of the Akumal aquifer was developed using the following procedure. From the

Table 1 Hydraulic heads at the specific sites of the study area

Site ID	Elevation (masl)
Uxuxubi	
W1	0.628
W2	0.930
W3	1.043
L1	1.091
L 2	0.954
Akumal village	
S1	0.785
S2	0.742

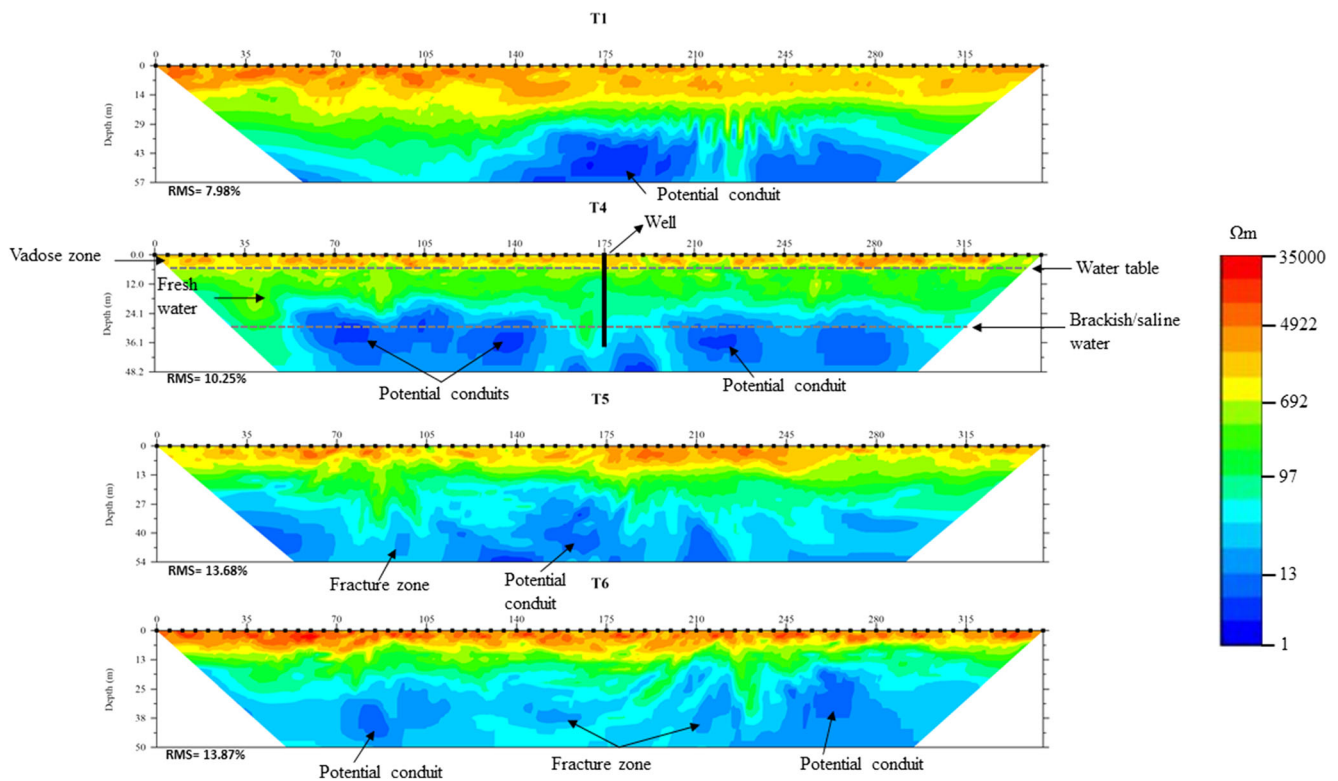


Fig. 4 ERT inverted sections obtained with the dipole-dipole array. All images have the same color scale

vertical profiles of groundwater EC, the depths of the following transition zones were obtained: (1) vadose/saturated with freshwater, (2) saturated with freshwater/blackish water and (3) saturated with blackish water/seawater. The values obtained for W3 and S3 can be seen in Table 2. Subsequently, the resistivity data of the inverted resistivity sections T2 and T4 were extracted at the depths indicated by their associated EC profiles; except for zone 3 in which the maximum resistivity value obtained from the inverted section T8 was used, because this transect was obtained at the beach line and the entire area was saturated with seawater. For the other zones, the resistivity values were extracted from strips of the following size: 345 m long (transect length) and 2.5 m thick (minimum precision of ERT measurements for a distance between electrodes of 5 m) at the indicated depths. The presented resistivity values for the transition zones are average values using data from both transects.

Transects T1, T2 and T6 were obtained approximately 6 km from the coast, while transects T3, T4 and T5 were obtained approximately 10 km from the coast, aligned in the same direction, and separated by a fracture, as can be seen in Fig. 2. From the inverted resistivity sections is observed a high-resistivity zone with values greater than 1,052 Ωm . These values correspond to the vadose zone of the aquifer according to the conceptual model of aquifer resistivity presented in Table 3.

Transect T8 was obtained on the beach sand, a few meters from the seawater edge (beach line), so the entire area is saturated with saltwater and presents resistivity values less than 7.3 Ωm . In the inverted section, two anomalies are observed below the surface at 225 and 315 m of the first electrode, which are associated with possible dissolution conduits or higher-porosity zones that give rise to groundwater discharges along the coast of the Mexican Caribbean (Null et al. 2014). Resistivity values of this transect, associated with a medium saturated with seawater, were used as a reference for the interpretation of the resistivity sections performed inland.

It is important to mention that structures referred to in this report as possible dissolution conduits are high-contrast areas, characterized by low-resistivity values with respect to the surrounding rock, but above the resistivity values reported for limestone rocks saturated with saltwater. In other areas of Yucatán Peninsula, values <100 Ωm have been reported for these structures (Andrade-Gómez et al. 2019).

Transect T7 was obtained inland, at 400 m from the beach line. The saturated zone with freshwater was observed, as well as the area saturated with saltwater. The latter was reached at 16 m deep and has resistivity values less than 10 Ωm . In addition, possible dissolution conduits were observed in the area saturated with saline water, approximately 20 m deep, which affect the thickness of the freshwater lens.

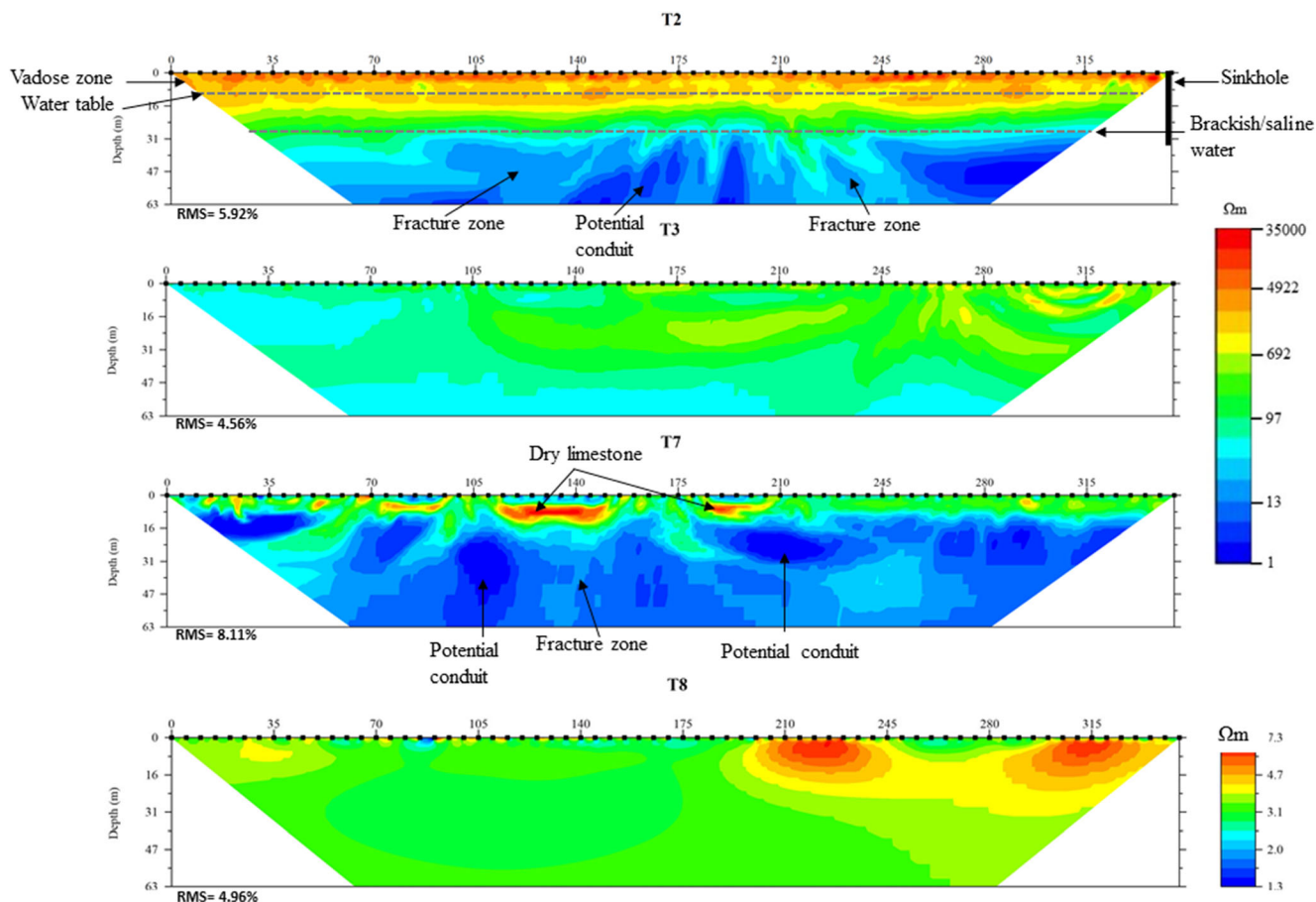


Fig. 5 ERT inverted sections obtained with the Wenner array. The color scale is the same as that used for the sections obtained with the dipole-dipole array, except for section T8

Transect T2 shows a layered behavior in terms of aquifer resistivity due to the Wenner type measurement: the vadose zone (red-yellow colours) with an approximate thickness of 16 m, the area saturated with freshwater (cyan-green colors) with a thickness of approximately 15 m, and below it, an area with presence of saline intrusion. In the latter area the presence of dissolution conduits and fractures can be observed. The identification of these structures was based on a comparison of the resistivity values obtained from the inversion process with those reported for similar structures in other areas of the Yucatán Peninsula karst aquifer, in which the same ERT technique was used (Andrade-Gómez et al. 2019). Sections T1 and T6 show greater lateral variability because they were obtained with the dipole-dipole array. For the T1 transect, in its middle section (175 m from the first sensor), an anomaly is observed

at 45 m depth, in the area saturated with saline water. On the other hand, in T6, two anomalies are observed, both in the area saturated with saline water. These anomalies can also be associated with the presence of dissolution conduits or flooded caverns and with the existence of fracture zones, since they present resistivity values similar to those previously reported for this karst aquifer (Andrade-Gómez et al. 2019).

Transects T4 and T5 have a similar inverted resistivity behavior, with a vadose zone with a thickness of approximately 6 m. In addition, it is appreciated that in both transects the thickness of the freshwater lens (cyan-green colors in Fig. 4) is variable, since it is affected by the dissolution conduits that are located over this area. In addition, both transects show the presence of saltwater intrusion with values less than 10 Ωm, at a depth of approximately 30 m.

Table 2 Depth to the transition zones of the aquifer as indicated by the EC profiles

Transition zone	Depth (m), from W3 profile	Depth (m), from S3 profile
Vadose/saturated with freshwater	4.774	10.96
Saturated with freshwater/blackish water	29.774	27.96
Blackish water/saturated with saltwater	34.774	32.96

Table 3 Conceptual resistivity model obtained from T2 and T4 ERT sections

Saturated zone	Resistivity (Ωm)
Vadose zone	>1,052
Carbonate saturated with freshwater	63–1,052
Carbonate saturated with blackish water	7.3–63
Carbonate saturated with saline water	<7.3

Transect T3 does not have resistivity values indicating the presence of saltwater intrusion according to the values developed for this area (Fig. 5), even though it is 400 m from transect T4. This indicates that the fracture between these two transects might be affecting the hydrogeological behavior of the aquifer. The color scale and its associated resistivity values indicate the saturation with freshwater of the entire area (Andrade-Gómez et al. 2019; Ochoa-Tinajero 2016).

Discussion

According to the results obtained in this work, it is noted that the fracture structure in the Uxuxubi site can be influencing groundwater behavior. This fracture acts, on a local scale, as a groundwater divide, which is evidenced by T3 and T4 sections. As a consequence of the barrier that forms this fracture, there is a change in flow direction at the local level, which is indicative of a microbasin (Steinich et al. 1996) as shown by the measurements obtained from the water table.

In addition, the values of the hydraulic heads obtained on a well close to the fracture (well W1 where the water table is located at 0.30 m below W2, W3, L1 and L2, as can be seen in Table 1), as indicated by the GPS positioning data, show significant variation compared to the nearby points. This is a clear indication that this fracture has a greater permeability and as a result there is a preferential flow over this area, as indicated by Tulaczyk et al. (1993) regarding the characteristic behavior of fractures found over the Holbox-Xel Ha fracture zone (regional behavior). The scale of this structure and its influence on the groundwater flow reinforces the possibility that this area behaves like a microbasin, with a boundary defined by this fracture.

According to Weidie (1978), on the surface of the Holbox-Xel Ha fracture, which is approximately 10 km parallel to the coast, there are poljes-type depressions, which are surface expressions (lagoons) characteristic of karst environments (Kranjc 2013). Measurements obtained at the L1 and L2 lagoons show the following important characteristics: (1) the lagoons are hydraulically connected, according to their heads with respect to sea level (0.941 and 0.954 m, respectively); (2) considering the water table measurements made in W2, it is

seen that these values also correspond to the same level of L1 and L2; therefore, they are also hydraulically connected; (3) T2 section shows that the area is completely saturated with freshwater up to a depth of 63 m. Therefore, based on the information obtained on this site, the lagoons found on the Uxuxubi site are not poljes, since they are a direct exposure of the Yucatán Peninsula aquifer; thus, it is more accurate to refer to them as karst depressions.

The values obtained for the hydraulic heads within the study area do not have variations greater than 4 cm, which is consistent with what was reported by Gondwe et al. 2010a, b, who mention that the hydraulic gradient in Yucatán Peninsula karst aquifer is less than 5 cm every 10 km. The obtained values reinforced the idea of a high hydraulic conductivity at the Pliocene coastal plains (Bauer-Gottwein et al. (2011).

The inverted resistivity transects T1, T2, T4, T5, and T6 show a three-layer pattern: a highly resistivity surface layer (resistivity greater than 1,052 Ωm), which is interpreted as the vadose area of the aquifer and is fractured. Note that this is characteristic of the area and matches what was shown in other works (Andrade-Gómez et al. 2019; Gómez-Nicolás et al. 2017; Ochoa-Tinajero 2016; Supper et al. 2009). A second layer is identified as the freshwater lens thickness of the aquifer according to the correlation of the values obtained from the EC profiles (Fig. 3). The lens is observed as an almost homogeneous layer according to the resistivity values shown in the T1 and T2 profiles, while in the T5 and T6 profiles there are significant variations in the freshwater lens. Finally, a third layer is identified as the saline intrusion zone with resistivity values less than 7.3 Ωm , which is observed up to a distance of 10 km from the coast in both the T4 and T5 resistivity sections and in the EC profile of the water column measured in the W3 well. However, the intrusion effect is no longer observed on T3 section. Again, this reinforces the idea and possibility that the fracture behaves like a barrier in this possible microbasin.

Additionally, possible dissolution conduits are observed in the T1, T5, T6 and T7 transects. It is important to note that ERT does not determine the direction of the dissolution conduits; however, given the alignment of the ERT, there is a possibility that the conduits found in T1 and T5 are oriented with the larger-scale fracture found on the east coast of Yucatán Peninsula (Holbox-Xel Ha fracture zone with south-west direction). This is consistent with Tulaczyk et al. (1993) who indicated that there is preferential flow at Yucatán Peninsula level on this fracture which influences the formation of this type of structure in this direction. In addition, dissolution conduits perpendicular to the coast are also observed in the T6, T7 and T8 transects. This observation is consistent with the values of the water levels in the area, which show that the flow within the microbasin is in the direction of the coast as indicated by Bauer-Gottwein et al. (2011).

The conduits found in the mixing zone (halocline) can be seen in the T1, T5 and T6 transects (Fig. 4). These conduits

affect the behavior of the halocline, since it is seen how there are variations in the halocline showing cones between dissolution conduits compared to what is observed in transect T2 (Fig. 5). This is possible because in the conduits there is greater permeability compared to the porous matrix, which results in water having a higher speed in these conduits and causing a pressure drop (Beddows 2004; Kambesis and Coke IV 2013).

Structural changes occur at varying depths (20–50 m), and these changes are observed at greater depths as one moves away from the coast. The depths to which the mixing area is found between freshwater and saltwater may be related to these structural changes (Collins et al. 2015). Since the mixing area is carbonate saturated, this leads to the dissolution of limestone rock (Beddows 2004) consequently influencing the formation of dissolution conduits (Smart et al. 2006). Transect T7 shows the clearest evidence of this process, taken 400 m from the coast, where a dissolution conduit is shown approximately 20 m deep.

In general, from the analysis of the inverted resistivity sections, a large presence of possible dissolution conduits forming a fractured network can be observed, which in addition to fractures at local scale, plays an important role in the behavior of groundwater flow.

Resistivity values interpreted as saline intrusion are lower than 10 Ωm , indicating a severe degree of intrusion where salinity ranges up to 25–30 mg/L (de Franco et al. 2009). Thus, for areas like Yucatán Peninsula where wells are scarce, ERT surveys with dipole-dipole and Wenner arrays are useful to identify seawater intrusion, and as mentioned earlier, karst features that influence the behavior of groundwater flows (Bauer-Gottwein et al. 2011; Gondwe et al. 2011).

The thicknesses of the freshwater lens measured at the two sites, with a distance between them of 4 km, show an important difference. The profile obtained at the site of Uxuxubi in May 2018 has a thickness of approximately 25 m, while the profile obtained in the area of Chemuyil measured in July 2018 has a thickness of 17 m. These values are consistent with the values measured by other researchers (Kovacs et al. 2017a, b; Moore et al. 1992) on the coast of the Mexican Caribbean, which show homogeneity in the freshwater lens in the karst-coastal aquifer of the Yucatán Peninsula. However, it is important to mention that this homogeneity is altered by the high density of structures identified as dissolution conduits and fractures areas, as can be seen from Figs. 4 and 5.

Accordingly, with the evaluation of the transects and borehole water EC profiles, it was possible to identify the stratified layers related to the structure of the Akumal area, as well the boundaries of the system promoted by the presence of a local fracture. Finally, the information obtained from this work could be used to generate a numerical model of groundwater flows, which would allow researchers to model the extent of the area (or zone) of seawater invasion near the coast, in a

similar way as has been reported for fractured coastal aquifers (Masciopinto et al. 2017). However, this last point is beyond the objectives of this work.

Conclusions

The general behavior of the aquifer in the Akumal area is similar to that observed in other regions of the Yucatán Peninsula. The structural information obtained from the ERT shows a highly resistive zone associated with the vadose zone, while in the saturated zone structural changes are observed with a strong presence of dissolution conduits, which affect the halocline shape. The saturated zone has a freshwater lens, relatively thin, with a maximum thickness of 25 at 10 km from the coast, diminishing as the distance to the coast decreases.

The general analysis of the ERT and hydraulic heads reinforced the idea that the Akumal area works hydrogeologically as a microbasin, where the exterior limit can be defined by a local fracture in the Uxuxubi site. It can be observed that this fracture acts, at a local scale, as a groundwater divide for groundwater flows; however, the general flow is still perpendicular to the coast.

According to these results, it is important that groundwater exploitation plans take into account the structural factors that control the availability of water resources, since these can affect the water availability, as in the presented case, where local structures create conditions of a possible microbasin. Information of this type can be obtained by applying the ERT technique, which has proven to be an invaluable tool for characterizing karst aquifers and for obtaining information that allows numerical modeling as well as the analysis of the aquifer vulnerability.

Acknowledgments The authors of this work acknowledge the contribution of Dr. Gilberto Acosta, M.C. Alejandro Carmona, Ing. Sarahí Del Angel Delgado, and Ing. Irving Escobedo Cen for the fieldwork. All authors appreciate the corrections made by the editor, associate editor, and reviewers to improve the original manuscript.

Funding J. C. Zamora-Luria thanks CONACyT for its financial support through the master grant No. 462886. J. A. Perera-Burgos and A. González-Calderón acknowledge the support provided by CONACYT: Cátedras CONACYT para jóvenes investigadores.

References

- Advanced Geosciences Inc (2005) Instruction manual for Earth-Imager 2D. Resistivity and IP inversion software. Advanced Geosciences, Austin, TX
- Advanced Geosciences Inc (2011) Instruction manual for SuperSting earth resistivity, IP & SP system PowerSting external high power transmitters. Advanced Geoscience, Austin
- Akumal PPDU (2007) Programa de Desarrollo Urbano Del Centro de Población Akumal 2007–2032 [Urban Development Program of

- Akumal Village 2007–2032]. Gobierno Municipal de Solidaridad, Quintana Roo, Mexico
- Andrade-Gómez L, Rebolledo-Vieyra M, Andrade JL, López PZ, Estrada-Contreras J (2019) Karstic aquifer structure from geoelectrical modeling in the ring of sinkholes, Mexico. *Hydrogeol J*. <https://doi.org/10.1007/s10040-019-02016-w>
- Bakalowicz M (2005) Karst groundwater: a challenge for new resources. *Hydrogeol J*. <https://doi.org/10.1007/s10040-004-0402-9>
- Bauer-Gottwein P, Gondwe BRN, Charvet G, Marín LE, Rebolledo-Vieyra M, Merediz-Alonso G (2011) Review: The Yucatán Peninsula karst aquifer, Mexico. *Hydrogeol J* 19(3):507–524. <https://doi.org/10.1007/s10040-010-0699-5>
- Beddows PA (2003) Cave hydrology of the Caribbean Yucatan coast. Association of Mexican Cave Studies Bulletin 1. AMCS, Austin, TX, 96 pp
- Beddows PA (2004) Groundwater hydrology of a coastal conduit carbonate aquifer: Caribbean coast of the Yucatán Peninsula, México. University of Bristol, Bristol, UK
- Beddows PA, Smart PL, Whitaker FF, Smith SL (2007) Decoupled fresh-saline groundwater circulation of a coastal carbonate aquifer: spatial patterns of temperature and specific electrical conductivity. *J Hydrol* 346(1–2):18–32. <https://doi.org/10.1016/j.jhydrol.2007.08.013>
- Bonet F, Butterlin J (1962) Stratigraphy of the northern part of the Yucatan Peninsula in Yucatan field trip guidebook. New Orleans Geological Society, New Orleans, LA, pp 52–57
- Canul-Macario C, Salles P, Hernández-Espriú A, Pacheco-Castro R (2020) Empirical relationships of groundwater head–salinity response to variations of sea level and vertical recharge in coastal confined karst aquifers. *Hydrogeol J*. <https://doi.org/10.1007/s10040-020-02151-9>
- Collins SV, Reinhardt EG, Rissolo D, Chatters JC, Nava Blank A, Luna Erreguerena P (2015) Reconstructing water level in Hoyo Negro, Quintana Roo, Mexico: implications for early Paleoamerican and faunal access. *Quat Sci Rev* 124:68–83. <https://doi.org/10.1016/j.quascirev.2015.06.024>
- CONAGUA (2002) Determinación de la Disponibilidad Del Agua en el Acuífero de la Península de Yucatán [Determination of the water availability at the Yucatan Peninsula Aquifer]. Secretaría de Medio Ambiente y Recursos Naturales, Mexico City, 20 pp
- CONAGUA (2014) Reporte del clima en México [Weather report in Mexico]. Secretaría de Medio Ambiente y Recursos Naturales, Mexico City, 27 pp
- Constable SC, Parker RL, Constable CG (1987) Occam's inversion: a practical algorithm for generating smooth models from electromagnetic sounding data. *Geophysics* 52(3):289. <https://doi.org/10.1190/1.1442303>
- Coutino A, Stastna M, Kovacs S, Reinhardt E (2017) Hurricanes Ingrid and Manuel (2013) and their impact on the salinity of the meteoric water mass, Quintana Roo, Mexico. *J Hydrol* 551:715–729. <https://doi.org/10.1016/j.jhydrol.2017.04.022>
- de Franco R, Biella G, Tosi L, Teatini P, Lozej A, Chiozzotto B, Giada M et al (2009) Monitoring the saltwater intrusion by time lapse electrical resistivity tomography: the Chioggia test site (Venice Lagoon, Italy). *J Appl Geophys* 69(3):117–130. <https://doi.org/10.1016/j.jappgeo.2009.08.004>
- Doro KO, Leven C, Círpka OA (2013) Delineating subsurface heterogeneity at a loop of River Steinlach using geophysical and hydrogeological methods. *Environ Earth Sci* 69:335–348. <https://doi.org/10.1007/s12665-013-2316-0>
- Escolero O, Marín LE, Steinich B, Pacheco JA, Anzaldo JM (2005) Geochemistry of the hydrogeological reserve of Mérida, Yucatán, Mexico. *Geofis Int* 44(3):301–314
- Ford DC, Williams PC (2007) Karst geomorphology and hydrology. Chapman and Hall, New York
- Galazoulas EC, Mertzaniides YC, Petalas CP, Kargiotis EK (2015) Large scale electrical resistivity tomography survey correlated to hydrogeological data for mapping groundwater salinization: a case study from a multilayered coastal aquifer in Rhodope, northeastern Greece. *Environ Proc* 2(1):19–35. <https://doi.org/10.1007/s40710-015-0061-y>
- García-Menéndez O, Ballesteros BJ, Renau-Pruñonosa A, Morell I (2018) Using electrical resistivity tomography to assess the effectiveness of managed aquifer recharge in a salinized coastal aquifer. *Environ Monit Assess* 190:19
- Goebel M, Pidlisecky A, Knight R (2017) Resistivity imaging reveals complex pattern of saltwater intrusion along Monterey coast. *J Hydrol* 551:746–755. <https://doi.org/10.1016/j.jhydrol.2017.02.037>
- Gómez-Nicolás M, Rebolledo-Vieyra M, Canto-Lugo E, Huerta-Quintanilla R, Ochoa-Sandoval P (2017) Connectivity in a karst system using electrical resistivity tomography and network theory. *Groundwater* 56(5):732–741. <https://doi.org/10.1111/gwat.12618>
- Gondwe BRN, Rahbek ML (2007) Modeling the groundwater catchment of the Sian Ka'an reserve, Quintana Roo. Association for Mexican Cave Studies, Austin, TX
- Gondwe BRN, Lerer S, Stisen S, Marín L, Rebolledo-Vieyra M, Merediz-Alonso G, Bauer-Gottwein P (2010a) Hydrogeology of the south-eastern Yucatan Peninsula: new insights from water level measurements, geochemistry, geophysics and remote sensing. *J Hydrol* 389(1–2):1–17. <https://doi.org/10.1016/j.jhydrol.2010.04.044>
- Gondwe BRN, Hong S-H, Wdowinski S, Bauer-Gottwein P (2010b) Hydrologic dynamics of the ground-water-dependent Sian Ka'an wetlands, Mexico, derived from InSAR and SAR data. *Wetlands* 30(1):1–13. <https://doi.org/10.1007/s13157-009-0016-z>
- Gondwe BRN, Merediz-Alonso G, Bauer-Gottwein P (2011) The influence of conceptual model uncertainty on management decisions for a groundwater-dependent ecosystem in karst. *J Hydrol* 400(1–2):24–40. <https://doi.org/10.1016/j.jhydrol.2011.01.023>
- Gondwe BRN, Ottowitz D, Supper R, Motschka K, Merediz-Alonso G, Bauer-Gottwein P (2012) Regional-scale airborne electromagnetic surveying of the Yucatan karst aquifer (Mexico): geological and hydrogeological interpretation. *Hydrogeol J* 20:1407–1425. <https://doi.org/10.1007/s10040-012-0877-8>
- Greggio N, Giambastiani B, Balugani E, Amaini C, Antonellini M (2018) High-resolution electrical resistivity tomography (ERT) to characterize the spatial extension of freshwater lenses in a salinized coastal aquifer. *Water* 10. <https://doi.org/10.3390/w10081067>
- Hartmann A, Goldscheider N, Wagener T, Lange J, Weiler M (2014) Karst water resources in a changing world: review of hydrological modeling approaches. *Rev Geophys* 1:218–242. <https://doi.org/10.1002/2013RG000443>. Received
- Hernández-Terrones LM, Null KA, Ortega-Camacho D, Payton A (2015) Water quality assessment in the Mexican Caribbean: impacts on the coastal ecosystem. *Cont Shelf Res* 102:62–72. <https://doi.org/10.1016/j.csr.2015.04.015>
- Instituto Nacional de Estadística y Geografía (2010) Número de habitantes, Quintana Roo [Number of habitants, Quintana Roo State]. <http://cuentame.inegi.org.mx/monografias/informacion/qroo/poblacion/>. Accessed 20 October 2018
- Isphording WC (1974) Weathering of Yucatan limestones: the genesis of Terra Rosas. In: Weidie AE (ed) Yucatan guidebook: New Orleans. New Orleans Geological Society, New Orleans LA, pp 78–93
- Kambesis PN, Coke IV JG (2013) Overview of the controls on eogenetic cave and karst development in Quintana Roo, Mexico. In: Lace M, Mylroide J (eds) Coastal karst landforms. Coastal research library, vol 5. Springer, Dordrecht, The Netherlands, pp 347–373. <https://doi.org/10.1007/978-94-007-5016-6>
- Ketabchi H, Mahmoodzadeh D, Ataie-Ashtiani B, Simmons CT (2016) Sea-level rise impacts on seawater intrusion in coastal aquifers: review and integration. *J Hydrol* 535:235–255. <https://doi.org/10.1016/j.jhydrol.2016.01.083>

- Kovacs SE, Reinhardt EG, Chatters JC, Rissolo D, Schwarcz HP, Collins SV, Kim S-T, Nava Blank A, Luna Erreguerena P (2017a) Calcite raft geochemistry as a hydrological proxy for Holocene aquifer conditions in Hoyo Negro and Ich Balam (Sac Actun cave system), Quintana Roo, Mexico. *Quat Sci Rev* 175:97–111. <https://doi.org/10.1016/j.quascirev.2017.09.006>
- Kovacs SE, Reinhardt EG, Stastna M, Coutino A, Werner C, Collins SV, Devos F, Le Maillot C (2017b) Hurricane Ingrid and Tropical Storm Hanna's effects on the salinity of the coastal aquifer, Quintana Roo, Mexico. *J Hydrol* 551:703–714. <https://doi.org/10.1016/j.jhydrol.2017.02.024>
- Kranjc A (2013) 6.10 Classification of closed depressions in carbonate karst. In: Shroder JF (ed) *Treatise on geomorphology*. Academic, San Diego, pp 104–111. <https://doi.org/10.1016/B978-0-12-374739-6.00125-1>
- Lauderdale RW, Ward WC, Weidie AE (1979) Carrillo Puerto Formation of northeastern Quintana Roo, Mexico. *Gulf Coast Assoc Geol Soc Trans* 29:275–280
- Leal-Bautista R, Lenczewski M, Morgan C, Gahala A, McClain J (2013) Assessing fecal contamination in groundwater from the Tulum region, Quintana Roo, Mexico *J Environ Prot* 4. <https://doi.org/10.4236/jep.2013.411148>
- Levanon E, Yechieli Y, Gvirtzman H, Shalev E (2017) Tide-induced fluctuations of salinity and groundwater level in unconfined aquifers: field measurements and numerical model. *J Hydrol* 551:665–675. <https://doi.org/10.1016/j.jhydrol.2016.12.045>
- López-Ramos E (1975) Geological summary of the Yucatan peninsula. In: Nairn AEM, Stehli FG (eds) *The ocean basins and margins*, vol 3: the Gulf of Mexico and the Caribbean. Plenum, New York, 26 pp
- Marín LE, Steinich B, Pacheco J, Escolero OA (2000) Hydrogeology of a contaminated sole-source karst aquifer. *Geofísica Internacional Universidad Nacional Autónoma de México Universidad Nacional Autónoma de México, Mérida, Yucatán*. *Geofis Int* 39(1):359–365
- Marín LE, Perry EC, Essaid HI, Steinich B (2004) Hydrogeological investigations and numerical simulation of groundwater flow in the karstic aquifer of northwestern Yucatan, México. In: Cheng A, Ouazar D (eds) *Coastal aquifer management-monitoring, modeling, and case studies*. CRC, Boca Raton, FL, pp 257–258
- Marino MA (1974) Rise and decline of the water table induced by vertical recharge. *J Hydrol* 23(3):289–298. [https://doi.org/10.1016/0022-1694\(74\)90009-2](https://doi.org/10.1016/0022-1694(74)90009-2)
- Masciopinto C, Liso I, Caputo MC, De Carlo L (2017) An integrated approach based on numerical modelling and geophysical survey to map groundwater salinity in fractured coastal aquifers. *Water* 9(11): 875. <https://doi.org/10.3390/w9110875>
- Medici G, West LJ, Chapman PJ, Banwart SA (2019) Prediction of contaminant transport in fractured carbonate aquifer types: a case study of the Permian Magnesian limestone group (NE England, UK). *Environ Sci Pollut Res* 26(24):24863–24884. <https://doi.org/10.1007/s11356-019-05525-z>
- Minsley BJ, Ajo-Franklin J, Mukhopadhyay A, Morgan FD (2011) Hydrogeophysical methods for analyzing aquifer storage and recovery systems. *Groundwater* 49(2):250–269. <https://doi.org/10.1111/j.1745-6584.2010.00676.x>
- Moore YH, Stoessell RK, Easley DH (1992) Fresh-water/sea-water relationship within a ground- water flow system, northeastern coast of the Yucatan Peninsula. *Ground Water* 3(3):343–350
- Null KA, Knee KL, Crook ED, de Sienes NR, Rebolledo-Vieyra M, Hernández-Terrones L, Paytan A (2014) Composition and fluxes of submarine groundwater along the Caribbean coast of the Yucatan Peninsula. *Cont Shelf Res* 77(7):38–50. <https://doi.org/10.1016/j.csr.2014.01.011>
- Ochoa-Tinajero, Luis E (2016) Inversión e Interpretación 2D y 3D de Datos de Resistividad Eléctrica En El Cenote Chac-Mool, Quintana Roo [Inversion and interpretation of 2D and 3D electrical resistivity data in the Cenote Chac-Mool, Quintana Roo]. Centro de Investigación Científica y de Educación Superior de Ensenada, Baja California
- Perry E, Marin L, McClain J, Velazquez G (1995) Ring of Cenotes (sinkholes), Northwest Yucatan, Mexico: its hydrogeologic characteristics and possible association with the Chicxulub Impact Crater. *Geology* 23(1):17–20. [https://doi.org/10.1130/0091-7613\(1995\)023<0017:ROCSNY>2.3.CO;2](https://doi.org/10.1130/0091-7613(1995)023<0017:ROCSNY>2.3.CO;2)
- Perry E, Velazquez-Oliman G, Marin L (2002) The hydrogeochemistry of the karst aquifer system of the Northern Yucatan Peninsula, Mexico. *Int Geol* 44(2):191–221. <https://doi.org/10.2747/0020-6814.44.3.191>
- Plank Z, Polg D (2019) Application of the DC resistivity method in urban geological problems of karstic areas. *Near Surf Geophys* 17:547–561. <https://doi.org/10.1002/nsg.12062>
- QRSS (2013) Quintana Roo Speleological Survey. www.caves.org/project/qrss.htm. Accessed 20 October 2018
- Rebolledo-Vieyra M, Urrutia-Fucugauchi J, Marin LE, Trejo-García A, Sharpton VL, Soler-Arechalde AM, (2010) UNAM Scientific Shallow-Drilling Program of the Chicxulub Impact Crater. *International Geology Review* 42 (10):928–940. <https://doi.org/10.1080/00206810009465118>
- Rebolledo-Vieyra M, Marin LE, Sharpton VL, Trejo-García A (2011) The Chicxulub impact crater and its influence on the regional hydrology in northwestern Yucatan, Mexico. In: Buster NA, Norris R (eds) *Gulf of Mexico origin, waters, and biota*, vol 3. Texas A&M University Press, College Station, TX, pp 279–290
- Redhaouania B, Aktarakçi H, Ountsche B, Gabtni H, Sami K, Bédir M (2015) Hydro-geophysical interpretation of fractured and karstified limestones reservoirs: a case study from Amdoun region (NW Tunisia) using electrical resistivity tomography, digital elevation model (DEM) and hydro-geochemical approaches. *J Afr Earth Sci* 112:328–338. <https://doi.org/10.1016/j.jafrearsci.2015.09.020>
- Redhaouania B, Ilondo BO, Gabtni H, Sami K, Bédir M (2016) Electrical resistivity tomography (ERT) applied to karst carbonate aquifers: case study from Amdoun, northwestern Tunisia. *Pure Appl Geophys* 173(4):1289–1303. <https://doi.org/10.1007/s00024-015-1173-z>
- Richards D, Richards S (2007) Overview of the geology and hydrology of coastal Quintana Roo, Mexico. *AMCS Activ Newslett* 30:104–109
- Saint-Loup R, Felix T, Maqueda A, Schiller A, Renard P (2018) A survey of groundwater quality in Tulum region, Yucatan Peninsula, Mexico. *Environ Earth Sci* 77. <https://doi.org/10.1007/s12665-018-7747-1>
- Schiller A, Supper R, Schattauer I, KMotschka K, Merediz Alonso G, López Tamayo A (2017) Advanced airborne electromagnetics for capturing hydrogeological parameters over the coastal karst system of Tulum, Mexico. *EuroKarst* 2016. <https://doi.org/10.1007/978-3-319-45465-8>
- Schönian F, Tagle R, Stöffler D, aKenkmann T (200) Geology of southern Quintana Roo (Mexico) and the Chicxulub ejecta blanket. 36th Lunar and Planetary Science Conference 2389. <http://www.liberlapidum.net/frank/frank.html>. Accessed September 2020
- Schulte P, Alegret L, Arenillas I, Arz JA, Barton PJ, Bown PR, Bralower TJ (2010) The Chicxulub asteroid impact and mass extinction at the Cretaceous-Paleogene boundary. *Science* 327(5970):1214–1218. <https://doi.org/10.1126/science.1177265>
- SGM (2006) Carta Geológico-minera cozumel F16-11 Quintana Roo [Geological-mineral map F16-11: Cozumel Quintana Roo Mexico]. SGM, Mexico City
- Sharma S, Verma GK (2015) Inversion of electrical resistivity data: a review. *Int J Environ Ecol Geol Geophys Eng* 9(4):400–406
- Smart P, Beddows P, Smith S, Whitaker F (2006) Cave development on the Caribbean Coast of the Yucatan Peninsula, Quintana Roo, Mexico. *Geological Soc Am Spec Pap* 404. [https://doi.org/10.1130/2006.2404\(10\)](https://doi.org/10.1130/2006.2404(10))

- Steinich B, Guadalupe VO, Marín LE, Perry E (1996) Determination of the ground water divide in the karst aquifer of Yucatán, Mexico, combining geochemical and hydrogeological data. *Geofis Int* 35(2): 153–159
- Stummer P, Maurer H, Green AG (2004) Experimental design: electrical resistivity data sets that provide optimum subsurface information. *Geophysics* 69(1):120–139. <https://doi.org/10.1190/1.1649381>
- Supper R, Motschka K, Ahl A, Bauer-Gottwein P, Gondwe B, Alonso GM, Römer A, Ottowitz D, Kinzelbach W (2009) Spatial mapping of submerged cave systems by means of airborne electromagnetics: an emerging technology to support protection of endangered karst aquifers. *Near Surf Geophys* 7(7):613–627. <https://doi.org/10.3997/1873-0604.2009008>
- Tassy A, Maxwell M, Borgomano J, Arfib B, Fournier F, Gilli E, Guglielmi Y (2014) Electrical resistivity tomography (ERT) of a coastal carbonate aquifer (Port-Miou, SE France). *Environ Earth Sci* 71(2):601–608. <https://doi.org/10.1007/s12665-013-2802-4>
- Telford WM, Geldart LP, Sheriff RE (1990) *Applied geophysics*, 2nd edn. Cambridge University Press, New York. <https://doi.org/10.1017/CBO9781139167932>
- Tulaczyk S M, Perry EC, Duller CE, Villasuso M (1993) Influence of the Holbox fracture zone on the karst geomorphology and hydrogeology of northern Quintana Roo, Yucatan Peninsula, Mexico. In: Proc 4th Multidisciplinary Conference on Sinkholes and the Engineering and Environmental Impacts of Karst, Panama City, Florida, 25–27 January 1993. Balkema, Rotterdam, The Netherlands, pp 181–188. [https://doi.org/10.1016/0148-9062\(94\)92835-5](https://doi.org/10.1016/0148-9062(94)92835-5)
- Vera I, Mariño-Tapia I, Enriquez C (2012) Effects of drought and subtidal sea-level variability on salt intrusion in a coastal karst aquifer. *Mar Freshw Res* 63(6):485–493. <https://doi.org/10.1071/MF11270>
- Wachniew P, Zurek AJ, Stumpp C, Gemitzi A, Gargini A, Filippini M, Rozanski K, Meeks J, Kværner J, Witczak S (2016) Toward operational methods for the assessment of intrinsic groundwater vulnerability: a review. *Crit Rev Environ Sci Technol* 46(9):827–884. <https://doi.org/10.1080/10643389.2016.1160816>
- Weidie AE (1978) Lineaments of the Yucatán Peninsula and fractures of the central Quintana Roo coast. In: Field trip no. 10-Yucatan, road log and supplement to 1978 Guidebook, 1982 GSA Annual Meeting, New Orleans, LA, pp 21–25
- Weidie AE (1985) Part I: geology of Yucatan platform. In: *Geology and hydrogeology of the Yucatan and Quaternary geology of northeastern Yucatan Peninsula*, pp 1–19. <http://archives.datapages.com/data/nogs/data/006/006007/0001.htm>
- Zhou W, Beck BF, Stephenson JB (2000) Reliability of dipole-dipole electrical resistivity tomography for defining depth to bedrock in covered karst terranes. *Environ Geol* 39(7):760–766. <https://doi.org/10.1007/s002540050491>
- Zhu J, Currens JC, Dinger JS (2011) Challenges of using electrical resistivity method to locate karst conduits: a field case in the Inner Bluegrass Region, Kentucky. *J Appl Geophys* 75(3):523–530. <https://doi.org/10.1016/j.jappgeo.2011.08.009>